Journal of Physics: Conference Series

PAPER • **OPEN ACCESS**

Experimental study: scour interference between vertical-wall abutment and two shape of bridge piers

To cite this article: N A Muhsen and S I Khassaf 2021 *J. Phys.: Conf. Ser.* **1973** 012044

Experimental study: scour interference between vertical-wall abutment and two shape of bridge piers

N A Muhsen[1] and S I Khassaf[2]

[1] Graduated Research Student, University of Basrah, Department of Civil Engineering, Basrah, Iraq.
[2] Professor, University of Basrah, Department of Civil Engineering, Basrah, Iraq.

emails:nooralbusiri@gmail.com

Abstract. Local scour considered as one of the main hazard factors that damaging bridges and in order to understand and controlling this problem, numerous researchers investigated its impact around pier or abutment in isolation but few take into account the consequences of pier proximity to abutment. This study aims to show the effect of pier-abutment scour interference. Under clear-water conditions, laboratory experiments were conducted utilizing vertical-wall abutment and two shape of pier (rectangular and ogival) at three different spacing (23.75, 16 and 9cm), and the influence of other parameters on reducing scouring process were also investigated. Approximately all results showed the increasing in pier scour depth with decreasing in abutment scour depth when reducing the spacing between them, where the maximum pier readings of scour depth was recorded at the smallest spacing. Also, scour increased with increasing flow intensity, Froude number and decreasing flow depth. Moreover, the maximum scour depth caused by rectangular shape was more than ogival shape by percentage about 11%.

1. Introduction

Scour process has a severe hazard to the performance and safety of the bridge structures over the world. Scour, collision and overloading are the three major problems which cause the failures of the bridge [1]. Scour can be defined as the result of a natural transportation phenomenon which occur due to natural flow changes or as a part of river morphology changes [2], while the depression left behind when sediment is carry away from the bed of the river by the flowing water is termed as the scour hole [3]. Whether during normal flow or flood events, the scour phenomenon can develop under any flow conditions, but its impact become higher during larger flow condition. The total scour at bridge composed of three components: general scour, contraction scour and local scour, and the last two components called localized scour [4].

The general scour refers to the changes in river bed elevation caused by lateral instability of the waterway. This type of scour can evolve irrespective of the existence of the bridge [5], and divided into long-term and short-term depending on the temporal development of the scour hole [6]. Short-term general scour develops due to a single or several closely spaced floods, while long-term develops completely over a longer time period [7]. Localized scour is directly attributable to the presence of a bridge contrary to general scour. The contraction scour known as the scour resulting from the acceleration of the flow due to a contraction [8]. This scour occurs due to a decrease in the channel width either naturally or due to the existence of a bridge.

The local scour occurs when the flow interferes with the bridge piers and abutments, which lead to an acceleration in the flow, creating vortices that can remove the bed material in the surrounding area of the bridge. Furthermore, local scour known as one of the major causes of bridge failures which led to a huge loss in life and economy, and resulted in severe impact on local transportation [9]. Figure 1 presents the types of scour developing around pier and abutment. The down-flow at the upstream face of the pier and abutment, and formation of subsequent horseshoe vortices at the base are known as the main mechanisms that causes scour at bridge pier and abutment [10].

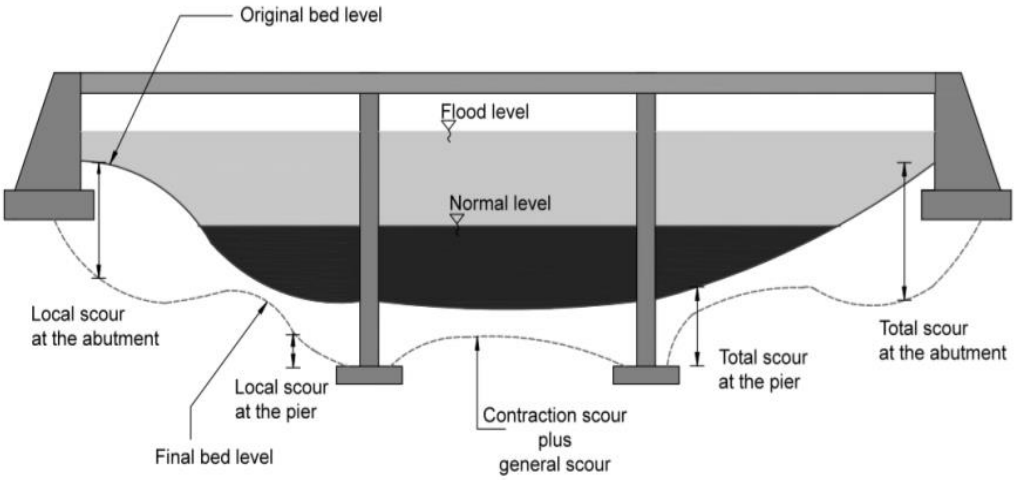

Figure 1. Types of scour around bridge pier and abutment [7].

2. Materials and methods

2.1. The experimental flume

The laboratory flume used in this research manufactured of fiberglass reinforced plastic material with steel reinforcement and have a recirculating closed water system with dimensions (5.64m x 0.61m x 0.4m) for length, width and depth, respectively (as shown in figure 2).

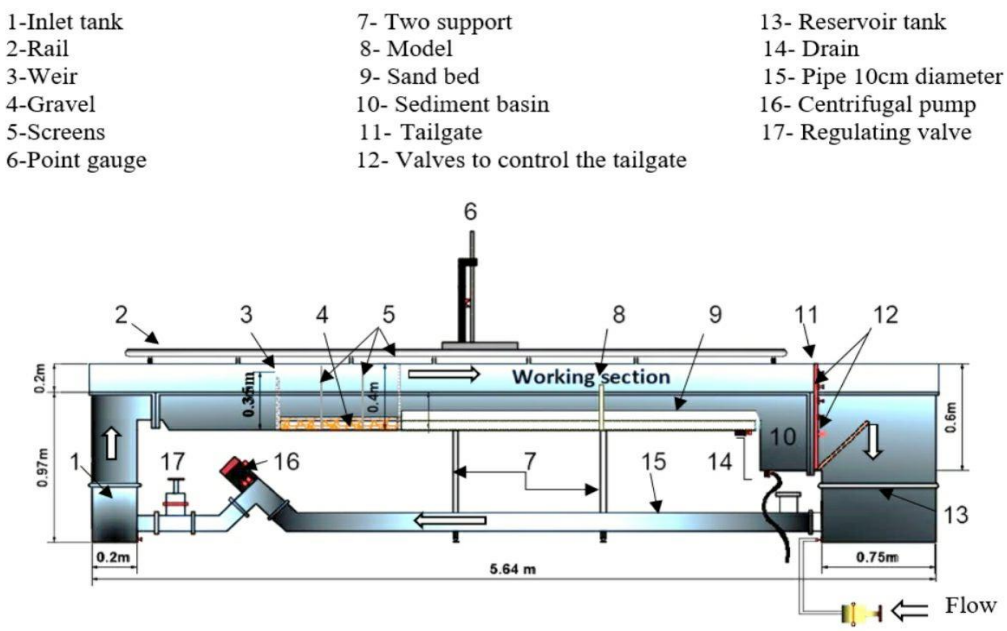

Figure 2. Schematic drawing of the flume with details.

The flume divided into three sections: the first contains an inlet tank located at the upstream side with (0.2m) length, (0.61m) width and depth of (1.17m). The working section represents the second section which contains a rectangular weir with (width=0.61m, height=0.35m), and three screens with gravel to prohibit any unfavourable particles and debris from entering the working section area. A layer of sand with (2.35m) length and (10cm) thickness was spread in the middle, and finally a sediment basin (length=0.4m, depth=0.3m) at the end of the section.
The third and last section is a reservoir at the downstream side with dimensions (0.75m x 0.61m x 1.17m) for length, width and depth, respectively. The reservoir used to supply water by a centrifugal pump connected with an electric motor having a maximum capacity of (8.5 l/sec). Water flow is controlled by a regulating valve, and all depth measurements in the flume are carried out by utilizing a point gauge having (±0.1mm reading accuracy) and move by a pair of parallel rails propped on the flume walls.

2.2. The experimental models
Physical models of pier and abutment were utilized; the models were made from plastic material with consideration that the surface for all models were smooth without any roughness. Two shape of pier (rectangular and ogival) were used having the same dimensions (width=3.5cm, length=7cm and height=20cm), in which the flume width is more than 8 times the pier size for clear-water conditions [11]. Also, a vertical-wall abutment was utilized in all experiments with (5cm) length, (7cm) width and (20cm) height (see figure 3 and 4).
All models were fixed vertically on the flume base and inner sidewall using adhesive material, and in the middle of the flume working section to obtain a well-established flow.

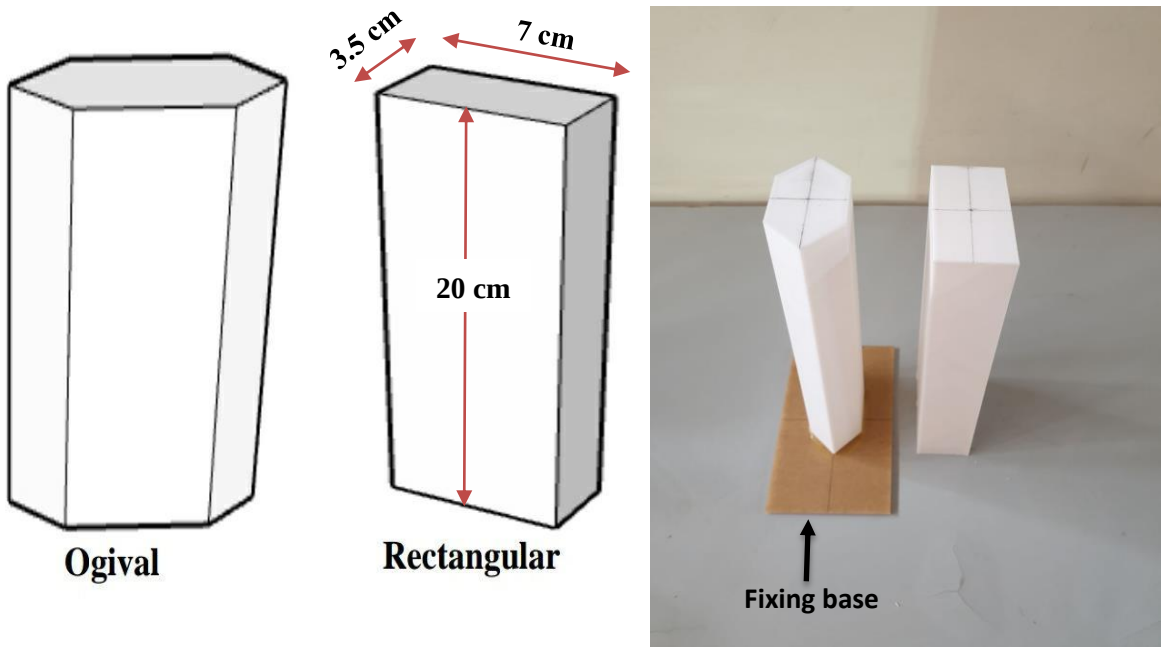

Figure 3. The pier models with a constant length to width ratio (l/b=2).

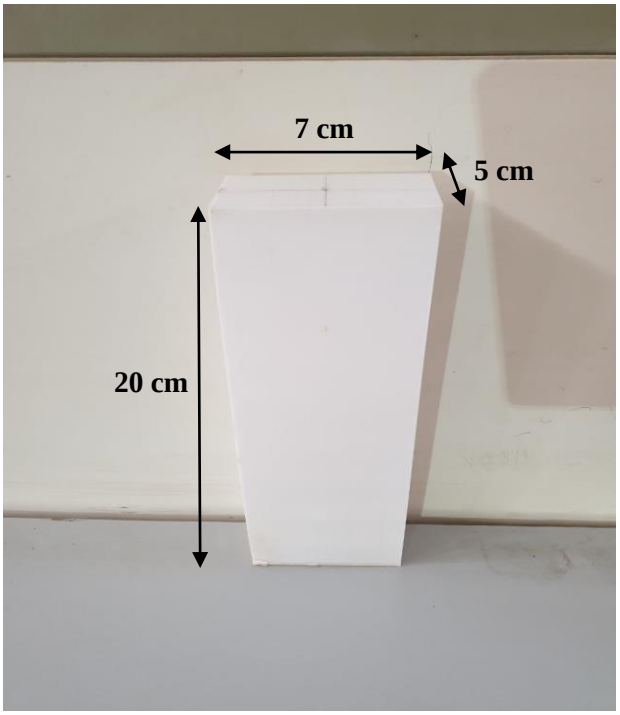

Figure 4. The physical vertical-wall abutment model.

2.3. The bed materials

For the purpose of classifying and obtain the characteristics of the sand bed material used in this study, mechanical sieve analysis was conducted at the soil laboratory in Civil Engineering Department, University of Basrah.

Based on the tests, the bed material consists of cohesionless sand with (d_{50}=0.3mm), where (d_{50}) is taken as median particle sediment size, and the geometric standard deviation (σ_g=1.32) was used to characterize the level of uniformity distribution particle size; where [$\sigma_g = (\frac{d_{85}}{d_{16}})^{1/2}$].

It is generally acceptable that the sediment probably considered as uniform if σ_g<1.4 and non-uniform else [12]. In figure 5, the approved specification is given as a distribution curve of grain size for bed material.

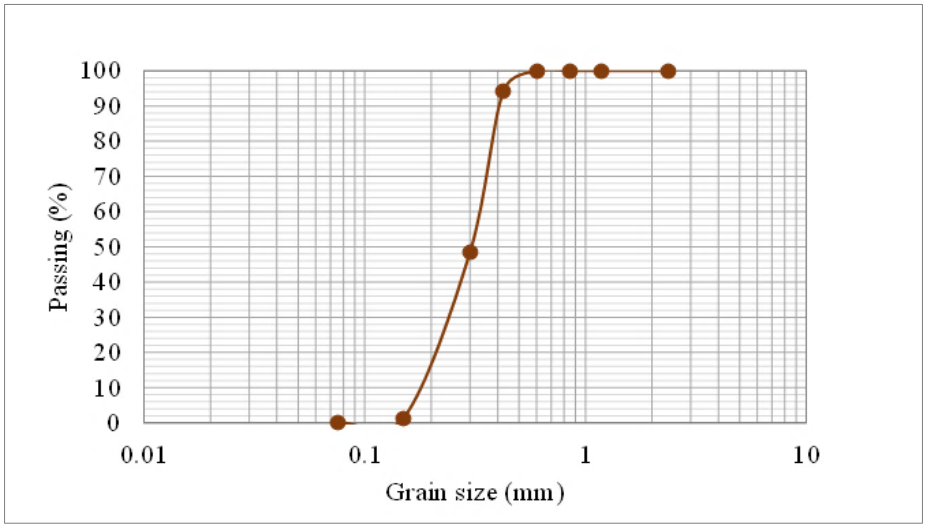

Figure 5. Distribution curve of grain size for bed material.

2.4. Classification of local scour and critical velocity

Local scour can be classified into two main types depending on the ability of the approaching flow to transport bed material, namely clear-water and live-bed scour [13].

In clear-water scour, the bed material is removed from the scour hole but not replenished by the approach flow (V ≤ Vc), and the maximum scour depth reached when the flow can no longer remove sediment particles from the scour hole. While in live-bed scour, the scour hole is continually refilled with sediment by the approach flow (V > Vc). Clear-water reaches its maximum value over a longer time period comparing with live-bed scour [14].

The critical mean velocity (Vc) and critical shear velocity (V^*c) were determined using the following equations [15]:

$$\frac{Vc}{V^*c} = 5.75\log(5.53\frac{y}{d_{50}}) \quad (1)$$

When 0.1mm < d_{50} < 1mm

$$V^*c = 0.0115 + 0.0125(d_{50})^{1.4} \quad (2)$$

Where: Vc= critical mean velocity, V^*c= Critical shear velocity for the median size, d_{50}= median diameter of bed size, y= flow depth.

2.5. Dimensional analysis

Dimensional analysis plays an effective role in illustrating the relationship between various physical quantities and can help in understanding the physical mechanism of scour process around pier and abutment. The local scour around pier and abutment depends on several parameters including flume parameters, pier and abutment parameters, fluid parameters, approaching flow parameters, and eventually the bed sediment parameters.

The maximum scour depth (ds_{max}) under clear-water conditions can be written as a function of the following variables:

$$ds_{max} = f\{B, S_\circ, b, L, X, \alpha, y, V, Vc, p_s, d_{50}, \sigma_g, p, \mu, g\} \quad (3)$$

$$\therefore f_1\{ds_{max}, B, S_\circ, b, L, X, \alpha, y, V, Vc, p_s, d_{50}, \sigma_g, p, \mu, g\} = 0 \quad (4)$$

The definition of these parameters are shown in table 1.

Table 1. The parameters affecting scour depth in (MLT) system.

Variables	Quantum	Dimensions
	Flume parameters	
B	Width of flume	L
$S_\circ$	Flume bed slope	-
	Pier and abutment parameters	
b	Pier or abutment width	L
L	Pier or abutment length	L
X	Spacing between pier and abutment (from face to face)	L
α	Angle of attack for pier and abutment	-
	Approaching flow parameters	
Y	Flow depth	L
V	Mean flow velocity	LT^{-1}
Vc	Critical velocity	LT^{-1}

Bed sediment parameters		
p_s	Sediment density	ML^{-3}
d_{50}	Median particle grain size	L
σ_g	Geometric standard deviation	-
Fluid parameters		
P	Fluid density	ML^{-3}
μ	Dynamic viscosity of fluid	$ML^{-1}T^{-1}$
g	Gravitational acceleration	LT^{-2}

The method of dimensional analysis used in this study is the Buckingham π-theorem.

$$\therefore 0 = f_2\left(\frac{ds_{max}}{y}, \frac{B}{y}, S_\circ, \frac{b}{y}, \frac{L}{y}, \frac{X}{y}, \alpha, \frac{V}{Vc}, \frac{p_s}{p}, \frac{d_{50}}{y}, \sigma_g, \frac{\mu}{pvy}, Fr\right) \quad (5)$$

Based on the conditions in this study, the impacts of these variables can be simplified according to the following hypothesis:

(1) The flume has constant bed width, thus the term $(\frac{B}{y})$ will be ignored.
(2) All runs were conducted under constant slope, since the flume has fixed horizontal slope ($S_\circ$=0). There was no impact of ($S_\circ$) on scour depth.
(3) The width and length were constant for all models, terms $(\frac{b}{y})$ and $(\frac{L}{y})$ will be negligible.
(4) All models aligned with the flow direction, thus eliminate (α) effect.
(5) Constant sediment size and relative density, thus effects of $(\frac{d_{50}}{y}, \frac{p_s}{p})$ were negligible.
(6) Steady viscosity was used, the effect of $(\frac{\mu}{pvy})$ was insignificant and ignored.

After eliminating the terms with constant value and has no effect on the scour process, the following equation can be obtained:

$$f_3\left(\frac{ds_{max}}{y}, \frac{X}{y}, \frac{V}{Vc}, Fr\right) = 0 \quad (6)$$

∴ The maximum scour depth:

$$\frac{ds_{max}}{y} = f_4\left(\frac{X}{y}, \frac{V}{Vc}, Fr\right) \quad (7)$$

This equation above and its variables will be used in laboratory experiments.

3. Results and Discussion

The discussion and analysis of results obtained from laboratory data is an essential step in designing the bridge, in order to reduce the impact of the scouring process. All the laboratory experiments were carried out in steady subcritical flow and clear-water conditions, and the results used in this study were recorded in table 2 and 3.

Table 2. Effect of spacing between pier and abutment at different flow velocities.

Rectangular pier with vertical-wall abutment							
Flow velocity (m/sec)	Flow depth (cm)	X=23.75cm		X=16cm		X=9cm	
		Pier ds (cm)	Abutment ds (cm)	Pier ds (cm)	Abutment ds (cm)	Pier ds (cm)	Abutment ds (cm)
0.118	3.5	2.7	1.8	3.15	1.85	3.55	1.5
0.139	3.5	3.9	2.65	4.6	2.35	4.55	1.9
0.159	3.5	4.48	2.9	4.78	2.75	5.05	2.6
0.165	3.5	4.7	3.1	4.85	2.85	5.1	2.9
0.176	3.5	5	3.7	5.25	3.3	5.35	3.05
Ogival pier with vertical-wall abutment							

0.118	3.5	2.05	1.3	2.25	1.35	2.8	1.5
0.139	3.5	3.2	2.45	3.45	2.2	3.6	1.85
0.159	3.5	3.8	2.85	4.05	2.55	4.25	2.3
0.165	3.5	4.1	3.5	4.25	2.75	4.4	2.5
0.176	3.5	4.45	3.6	4.6	3.1	4.75	2.8

Table 3. The experimental results for all models.

Run No.	X (cm)	Y (cm)	Q $(\frac{L}{sec})$	V $(\frac{m}{sec})$	Vc $(\frac{m}{sec})$	Fr	$\frac{V}{Vc}$	$\frac{X}{y}$	Pier ds (cm)	$\frac{ds}{y}$	Abutment ds (cm)	$\frac{ds}{y}$
Rectangular pier with vertical-wall abutment												
1	23.75	3.5	2.527	0.118	0.223	0.201	0.529	6.785	2.7	0.77	1.8	0.51
2	23.75	3.5	2.977	0.139	0.223	0.237	0.623	6.785	3.9	1.11	2.65	0.76
3	23.75	3.5	3.401	0.159	0.223	0.271	0.713	6.785	4.48	1.28	2.9	0.83
4	23.75	3.5	3.524	0.165	0.223	0.281	0.740	6.785	4.7	1.34	3.1	0.89
5	23.75	3.5	3.770	0.176	0.223	0.30	0.789	6.785	5	1.43	3.7	1.06
6	23.75	3	3.770	0.206	0.217	0.379	0.949	7.916	5.35	1.78	4.25	1.42
7	23.75	4	3.770	0.154	0.227	0.245	0.678	5.937	4.25	1.06	3.15	0.79
8	23.75	4.5	3.770	0.137	0.231	0.206	0.593	5.277	3.5	0.78	2.65	0.59
9	23.75	5	3.770	0.123	0.235	0.175	0.523	4.750	3.3	0.66	2.38	0.48
10	16	3.5	2.527	0.118	0.223	0.201	0.529	4.571	3.15	0.9	1.85	0.53
11	16	3.5	2.977	0.139	0.223	0.237	0.623	4.571	4.6	1.31	2.35	0.67
12	16	3.5	3.401	0.159	0.223	0.271	0.713	4.571	4.78	1.37	2.75	0.79
13	16	3.5	3.524	0.165	0.223	0.281	0.740	4.571	4.85	1.39	2.85	0.81
14	16	3.5	3.770	0.176	0.223	0.30	0.789	4.571	5.25	1.50	3.3	0.94
15	16	3	3.770	0.206	0.217	0.379	0.949	5.333	5.45	1.82	3.6	1.20
16	16	4	3.770	0.154	0.227	0.245	0.678	4.0	4.48	1.12	3.1	0.78
17	16	4.5	3.770	0.137	0.231	0.206	0.593	3.555	3.3	0.73	2.7	0.60
18	16	5	3.770	0.123	0.235	0.175	0.523	3.20	3.05	0.61	2.35	0.47
19	9	3.5	2.527	0.118	0.223	0.201	0.529	2.571	3.55	1.01	1.5	0.43
20	9	3.5	2.977	0.139	0.223	0.237	0.623	2.571	4.55	1.30	1.9	0.54
21	9	3.5	3.401	0.159	0.223	0.271	0.713	2.571	5.05	1.44	2.6	0.74
22	9	3.5	3.524	0.165	0.223	0.281	0.740	2.571	5.1	1.46	2.9	0.83
23	9	3.5	3.770	0.176	0.223	0.30	0.789	2.571	5.35	1.53	3.05	0.87
24	9	3	3.770	0.206	0.217	0.379	0.949	3.0	5.7	1.90	3.15	1.05
25	9	4	3.770	0.154	0.227	0.245	0.678	2.250	4.7	1.18	2.9	0.73
26	9	4.5	3.770	0.137	0.231	0.206	0.593	2.0	3.7	0.82	2.75	0.61
27	9	5	3.770	0.123	0.235	0.175	0.523	1.80	3	0.60	2.6	0.52
Ogival pier with vertical-wall abutment												
28	23.75	3.5	2.527	0.118	0.223	0.201	0.529	6.785	2.05	0.59	1.3	0.37
29	23.75	3.5	2.977	0.139	0.223	0.237	0.623	6.785	3.2	0.91	2.45	0.70
30	23.75	3.5	3.401	0.159	0.223	0.271	0.713	6.785	3.8	1.09	2.85	0.81
31	23.75	3.5	3.524	0.165	0.223	0.281	0.740	6.785	4.1	1.17	3.5	1.0
32	23.75	3.5	3.770	0.176	0.223	0.30	0.789	6.785	4.45	1.27	3.6	1.03
33	23.75	3	3.770	0.206	0.217	0.379	0.949	7.916	4.8	1.60	4.2	1.40
34	23.75	4	3.770	0.154	0.227	0.245	0.678	5.937	3.5	0.88	2.8	0.70
35	23.75	4.5	3.770	0.137	0.231	0.206	0.593	5.277	2.85	0.63	2.7	0.60
36	23.75	5	3.770	0.123	0.235	0.175	0.523	4.750	2.3	0.46	2.65	0.53
37	16	3.5	2.527	0.118	0.223	0.201	0.529	4.571	2.25	0.64	1.35	0.39
38	16	3.5	2.977	0.139	0.223	0.237	0.623	4.571	3.45	0.99	2.2	0.63
39	16	3.5	3.401	0.159	0.223	0.271	0.713	4.571	4.05	1.16	2.55	0.73

40	16	3.5	3.524	0.165	0.223	0.281	0.740	4.571	4.25	1.21	2.75	0.79
41	16	3.5	3.770	0.176	0.223	0.30	0.789	4.571	4.6	1.31	3.1	0.89
42	16	3	3.770	0.206	0.217	0.379	0.949	5.333	4.85	1.62	3.7	1.23
43	16	4	3.770	0.154	0.227	0.245	0.678	4.0	3.85	0.96	2.7	0.68
44	16	4.5	3.770	0.137	0.231	0.206	0.593	3.555	2.7	0.60	2.6	0.58
45	16	5	3.770	0.123	0.235	0.175	0.523	3.20	2	0.40	2.4	0.48
46	9	3.5	2.527	0.118	0.223	0.201	0.529	2.571	2.8	0.80	1.5	0.43
47	9	3.5	2.977	0.139	0.223	0.237	0.623	2.571	3.6	1.03	1.85	0.53
48	9	3.5	3.401	0.159	0.223	0.271	0.713	2.571	4.25	1.21	2.3	0.66
49	9	3.5	3.524	0.165	0.223	0.281	0.740	2.571	4.4	1.26	2.5	0.71
50	9	3.5	3.770	0.176	0.223	0.30	0.789	2.571	4.75	1.36	2.8	0.80
51	9	3	3.770	0.206	0.217	0.379	0.949	3.0	4.9	1.63	4.2	1.40
52	9	4	3.770	0.154	0.227	0.245	0.678	2.250	3.9	0.98	2.3	0.58
53	9	4.5	3.770	0.137	0.231	0.206	0.593	2.0	2.8	0.62	2.25	0.50
54	9	5	3.770	0.123	0.235	0.175	0.523	1.80	2.25	0.45	2.18	0.44

3.1. Effect of flow intensity ($\frac{V}{Vc}$) on the local scour ($\frac{ds}{y}$)

The flow intensity parameter has a significant influence on the depth of scour. Sets of experiments were conducted to confirm the relationship between the scour depth ratio and the flow intensity at 5 different velocities for each pier shape while all the other parameters remain constant. From the results shown in figure 6, it can be noticed that the depth of scour ratio is increasing linearly with the increasing in flow intensity around pier and abutment for velocities beneath the threshold value.

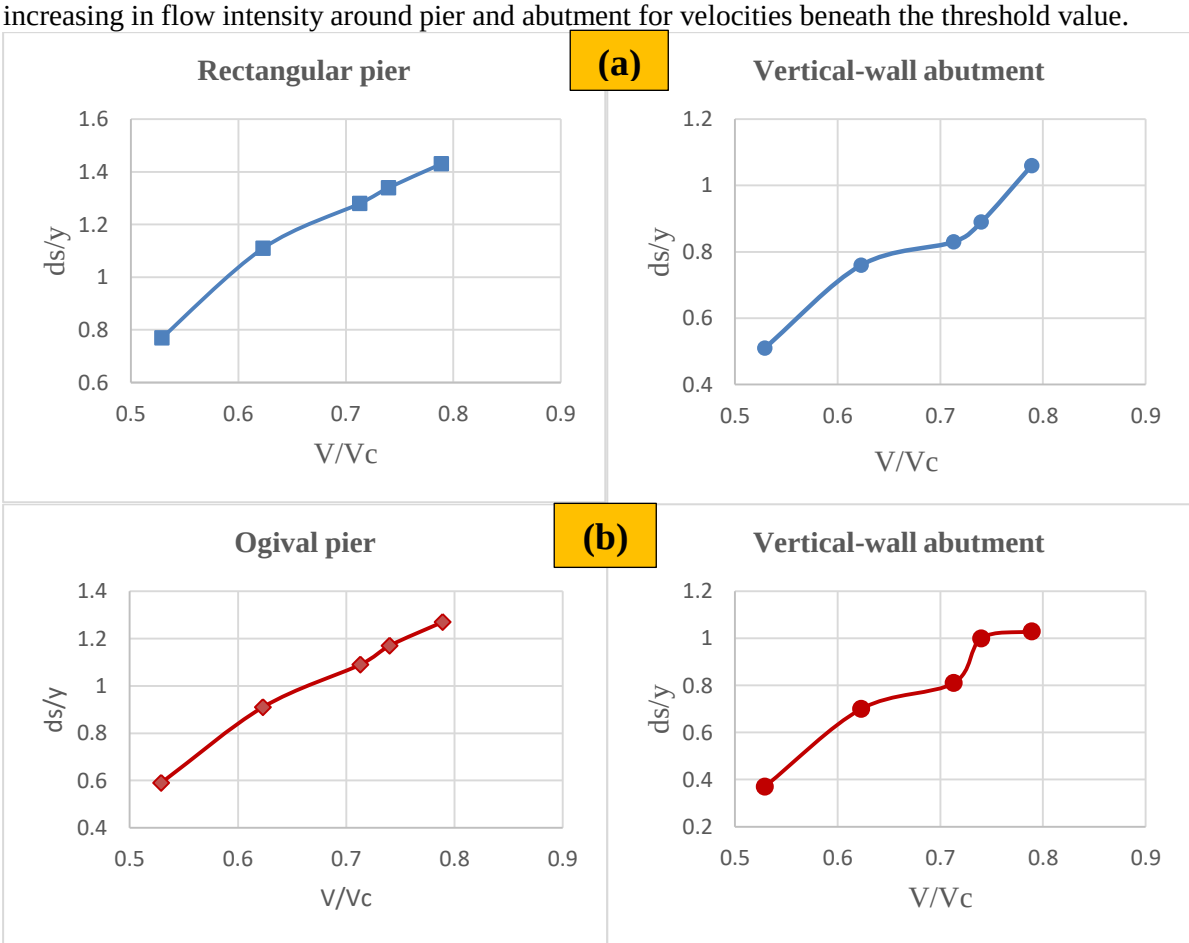

Figure 6. Effect of flow intensity on the scour depth ratio at (y=3.5cm and X=23.75cm) for (a) Rectangular pier with abutment and (b) Ogival pier with abutment.

Some photos of the laboratory experiments were chosen to show the scour process, as presented in figure 7. Thus, it can be observed that: the volume and width of the scour depth will increase due to the increase in separation region by increasing flow intensity, and as a result create more eddies which in turn cause more scour.

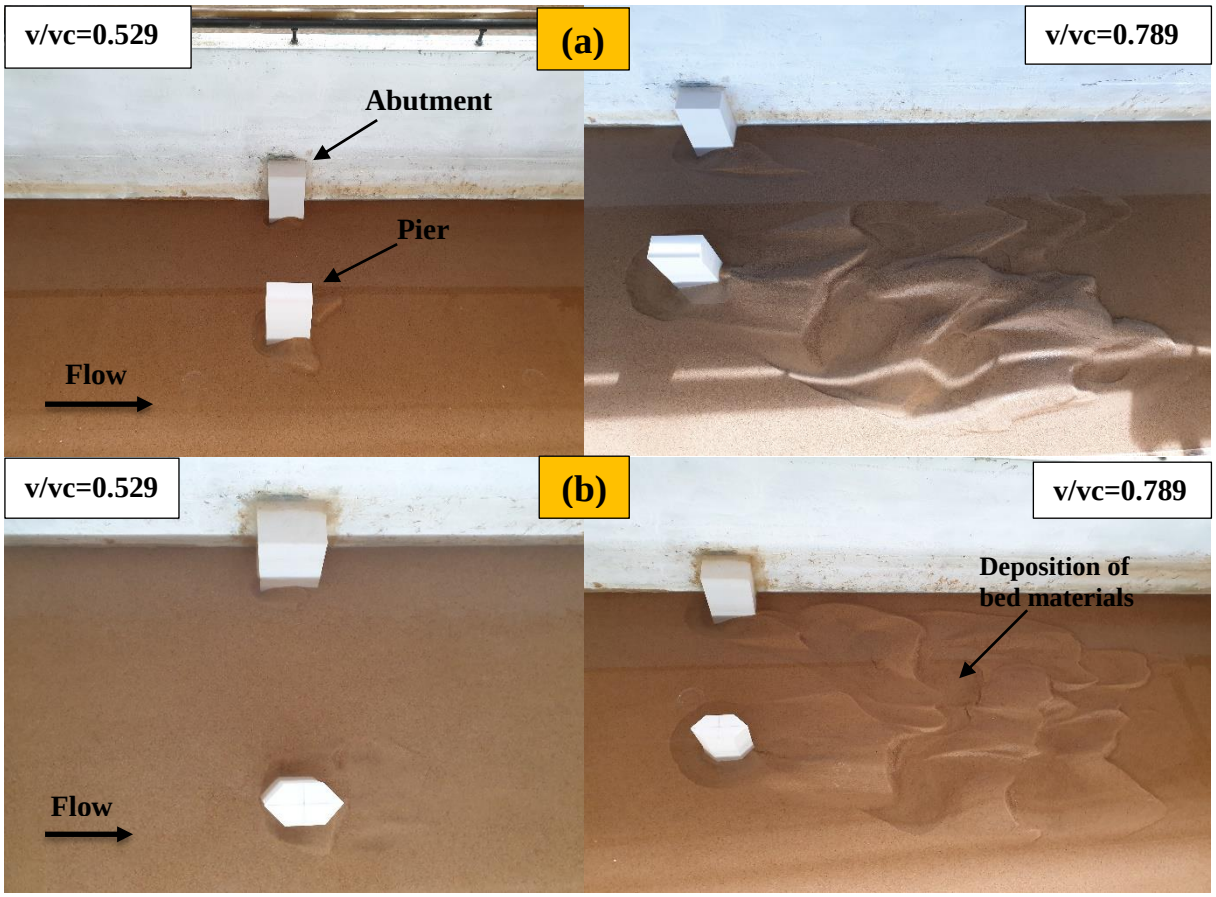

Figure 7. Photos that illustrate the effect of flow intensity on the development of scour depth ratio for (a) rectangular pier with abutment and (b) ogival pier with abutment.

3.2. Effect of Froude number (Fr) on the local scour ($\frac{ds}{y}$)

Froude number considered as one of the main parameters that affect the scour process around pier and abutment. Laboratory experiments were carried out to show the influence of this parameter on scour depth ratio ($\frac{ds}{y}$), the acquired results were presented in figure 8.

The conclusion from the figure that, the depth of scour will increase with increasing Froude number. This can be explained based on Froude number law ($Fr = \frac{v}{\sqrt{gy}}$) which show that the increasing in flow velocity (V) versus an increasing in Froude number (Fr) and thus, this will lead to an increase in the scour depth ratio at a constant flow depth (y).

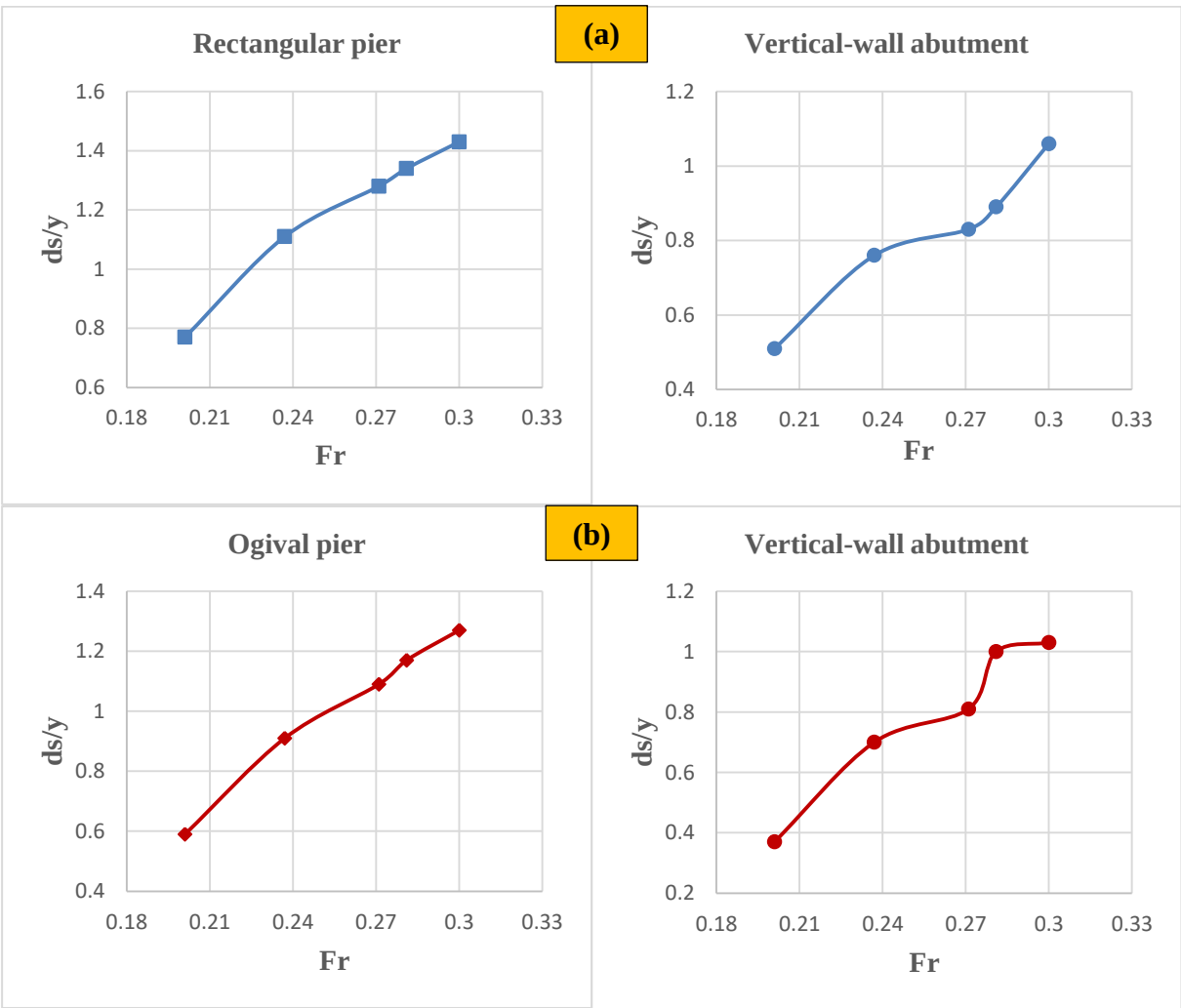

Figure 8. Effect of Froude number (Fr) on scour depth ratio at (y=3.5cm and X=23.75cm) for (a) rectangular pier with abutment and (b) ogival pier with abutment.

In addition, figure 9 shows the impact of Froude number increasing on the scour process in the laboratory.

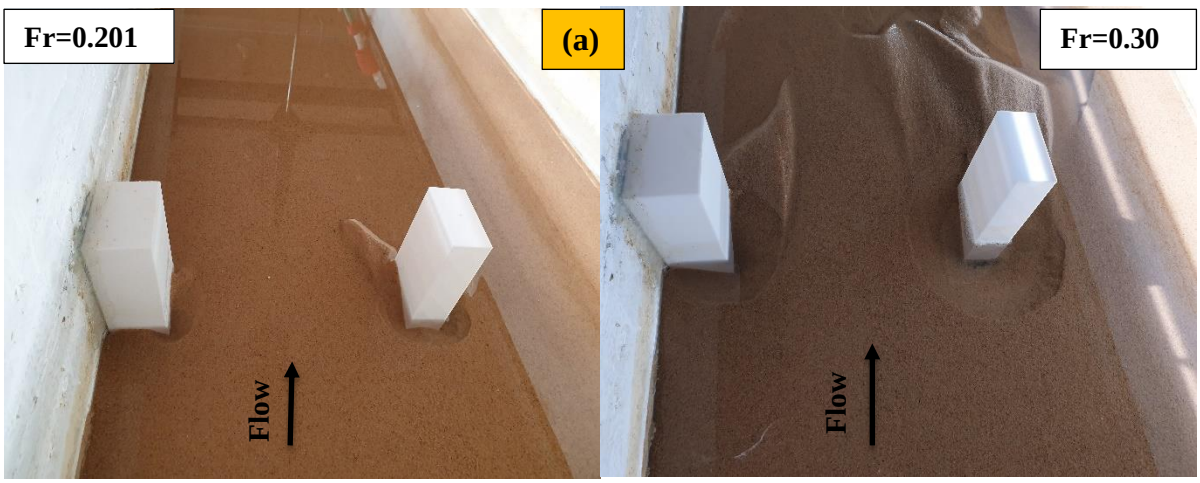

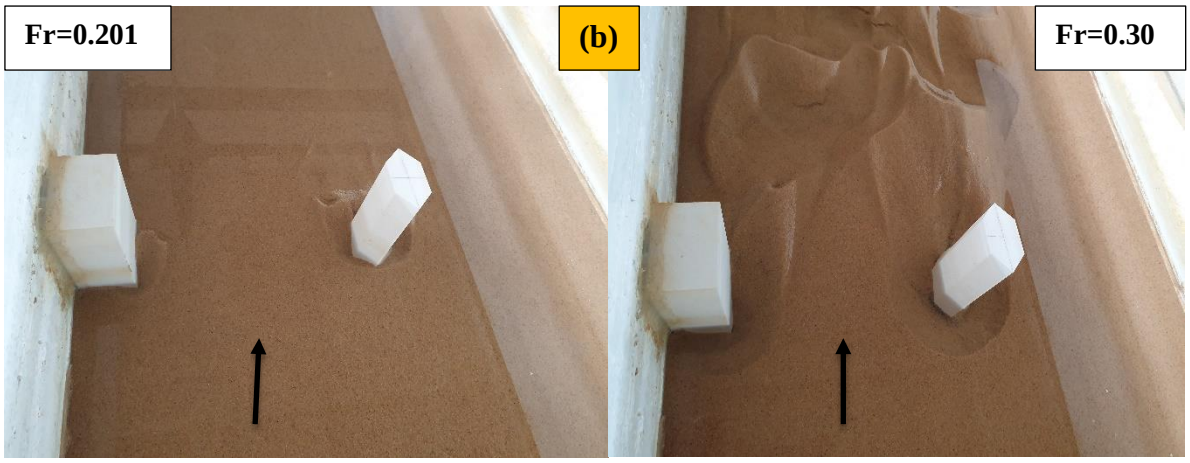

Figure 9. Photos to show the effect of Froude number (Fr) on the scour depth ratio at (X=23.75cm and y=3.5cm) for (a) rectangular pier with abutment and (b) ogival pier with abutment.

3.3. Effect of spacing between pier and abutment ($\frac{X}{y}$) on the local scour ($\frac{ds}{y}$)

Spacing is one of the parameters that affect the scour geometry around pier and abutment. Sets of experiments were carried out at 3 different distances (x) between pier and abutment to show the impact of spacing on scour depth. The obtained results were plotted in figure 10 to relate the spacing between pier and abutment ($\frac{X}{y}$) with the scour depth ratio ($\frac{ds}{y}$).

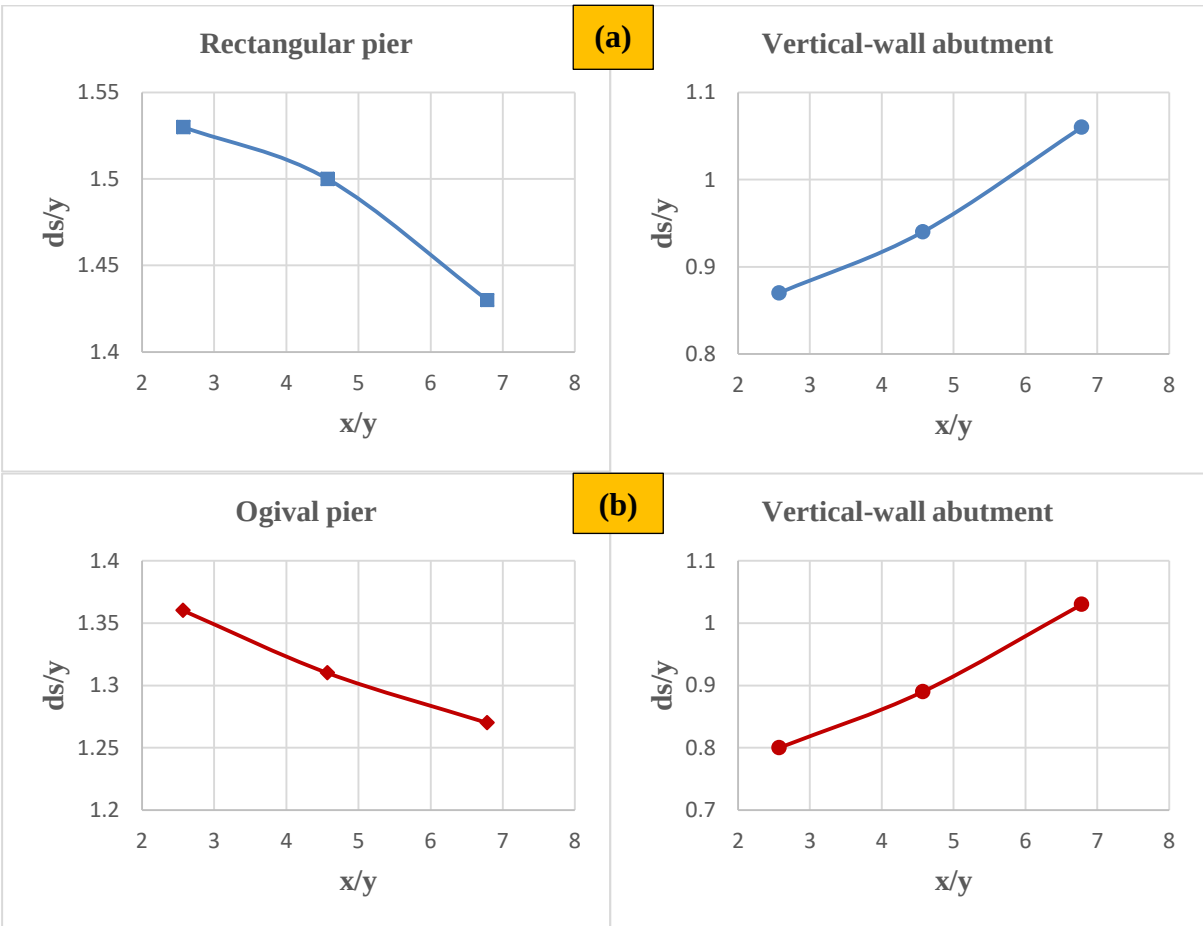

Figure 10. Effect of spacing between pier and abutment on the development of the scour depth ratio at (V=0.176m/sec and y=3.5cm) for (a) rectangular pier and abutment and (b) ogival pier and abutment.

From the figure above it can be concluded that when increasing the spacing between pier and abutment, the development of scour depth in almost all experiments become lower for piers and higher for abutment. The increasing percentage in the scour depth was measured to be (5%) and (3.4%) for rectangular and ogival pier, respectively when reducing the spacing from (X=23.75 to 16cm). While when reducing spacing from (X=23.75 to 9cm), the increasing percentage was (7%) for rectangular and (6.7%) for ogival pier. Furthermore, the decreasing percentage in the scour hole for vertical-wall abutment was ranged between (10.8-13.9) % and (17.6-22.2) % when reducing the spacing from (23.75 to 16cm) and (23.75 to 9cm), respectively. This is due to the interference between horseshoe vortex of the two structures. When reduce the spacing, the scour holes of pier and abutment will interfere together and causes filling of sediment particle for abutment, as a result the scour depth for abutment will be reduced. Figure 11 and 12 presented some photos of reducing distance between pier and abutment. Also more details about the spacing parameter effect shown in table 2.

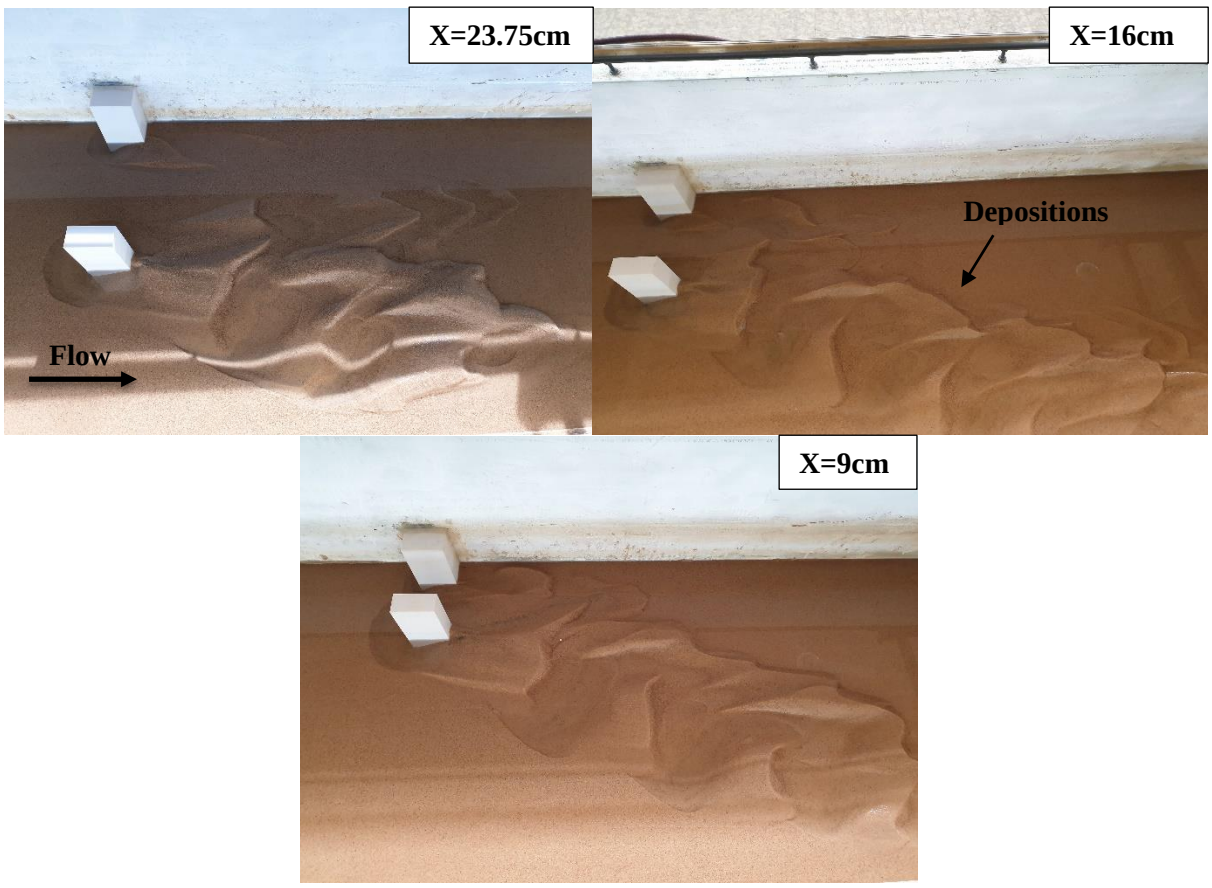

Figure 11. Effect of spacing between pier and abutment (x) on local scour depth for rectangular pier at (V=0.176 m/sec and y=3.5cm).

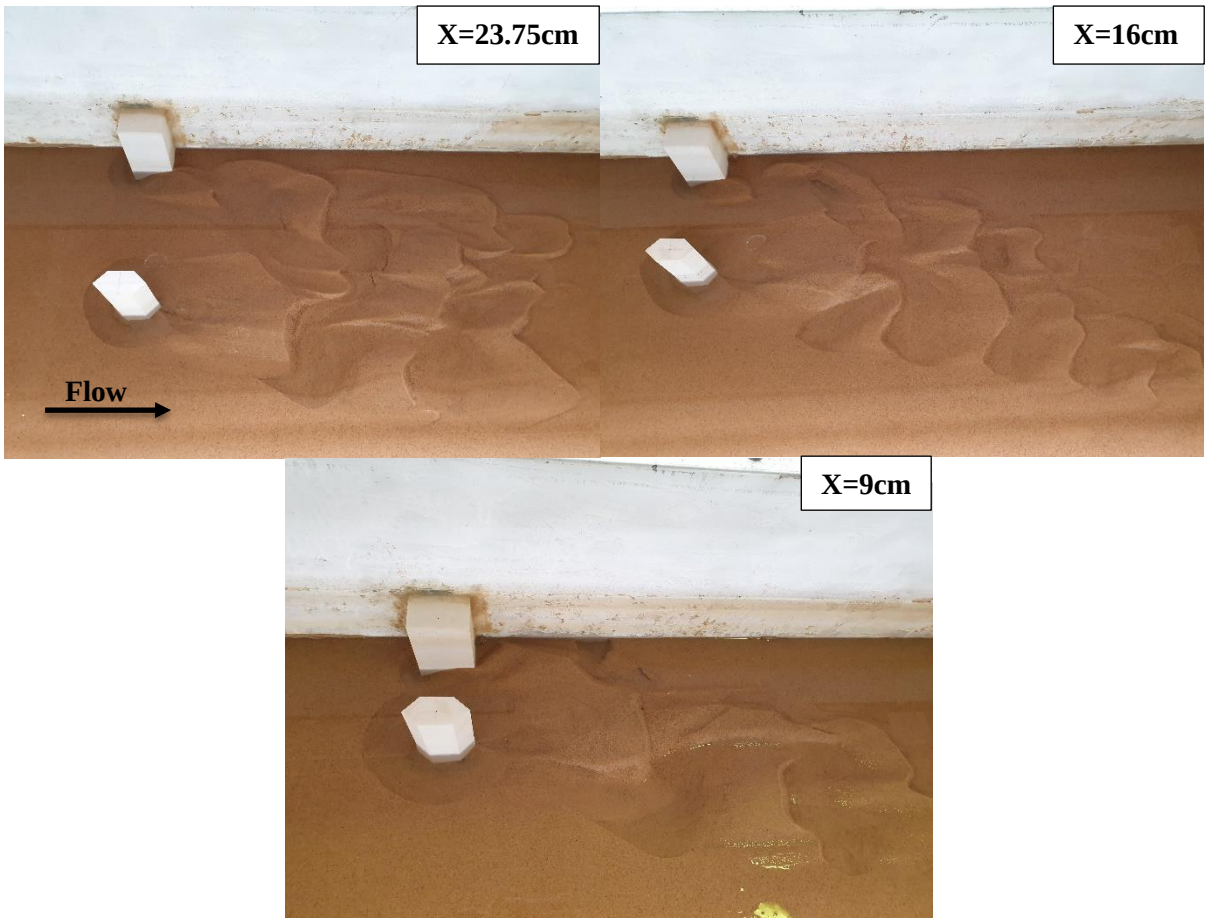

Figure 12. Effect of spacing between pier and abutment (X) on the local scour depth for ogival pier at (V=0.176 m/sec and y=3.5cm).

3.4. Effect of flow depth (y) on the local scour depth (ds)

To clarify the impact of flow depth on the scouring process, a number of laboratory experiments utilized to show this effect and the obtained results were illustrated in figure 13.

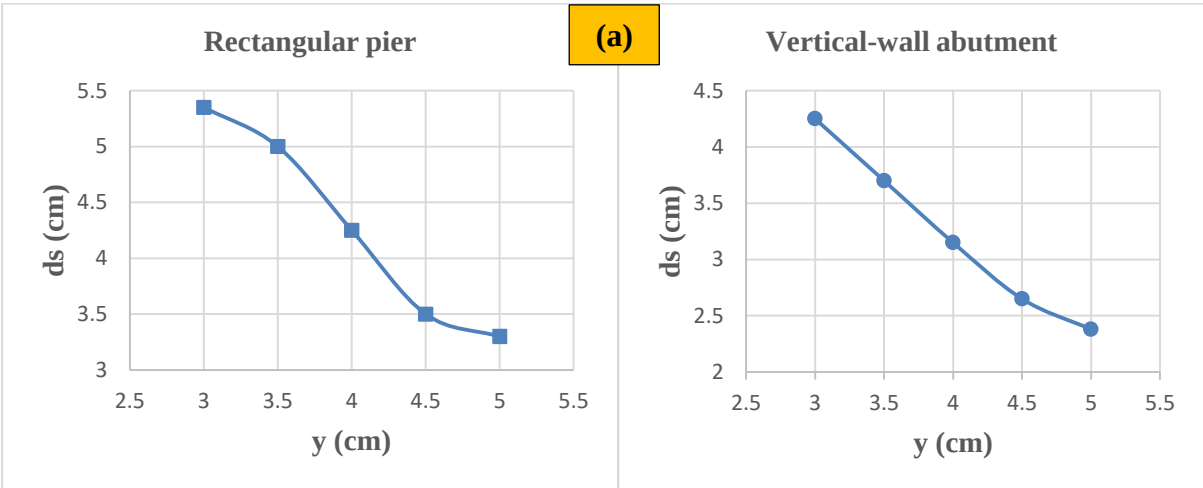

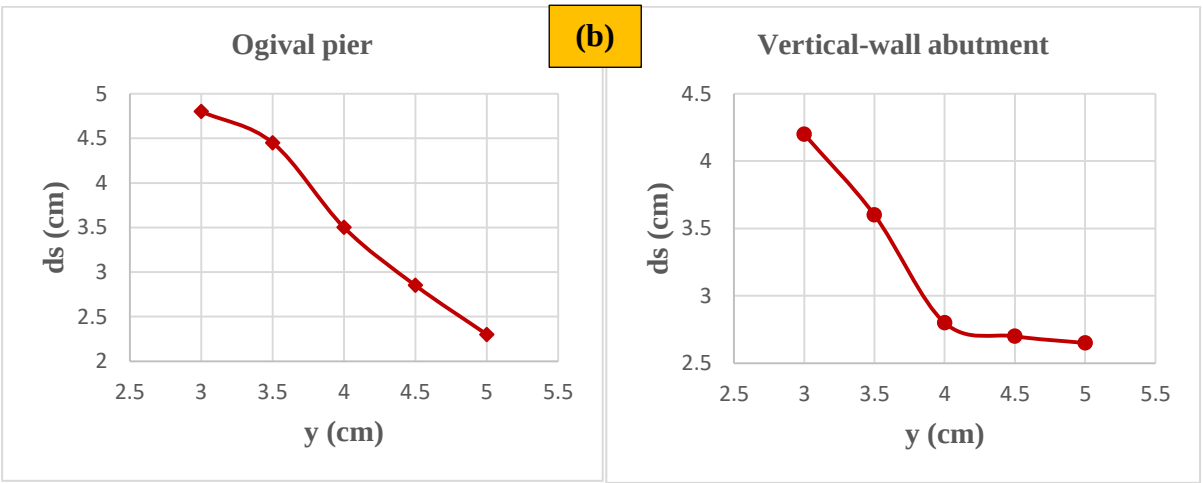

Figure 13. Effect of flow depth (y) on the depth of scouring process (ds) at spacing of (X=23.75cm) for (a) rectangular pier with abutment and (b) ogival pier with abutment.

The figure above shown that the flow depth (y) is inversely proportional to the scour depth, in which under the same flow condition as long as the flow depth is increasing, the scour depth will decrease. This is due to the practically absent of the re-circulating motions near the free surface when increasing the flow depth, thus causing the decrease of horseshoe vortices ability to pick up and entrain sediment (i.e. the surface roller will interfere with horseshoe vortex when decreasing flow depth, thus causing more scour of bed sediment). Some photos for this case shown in figure 14.

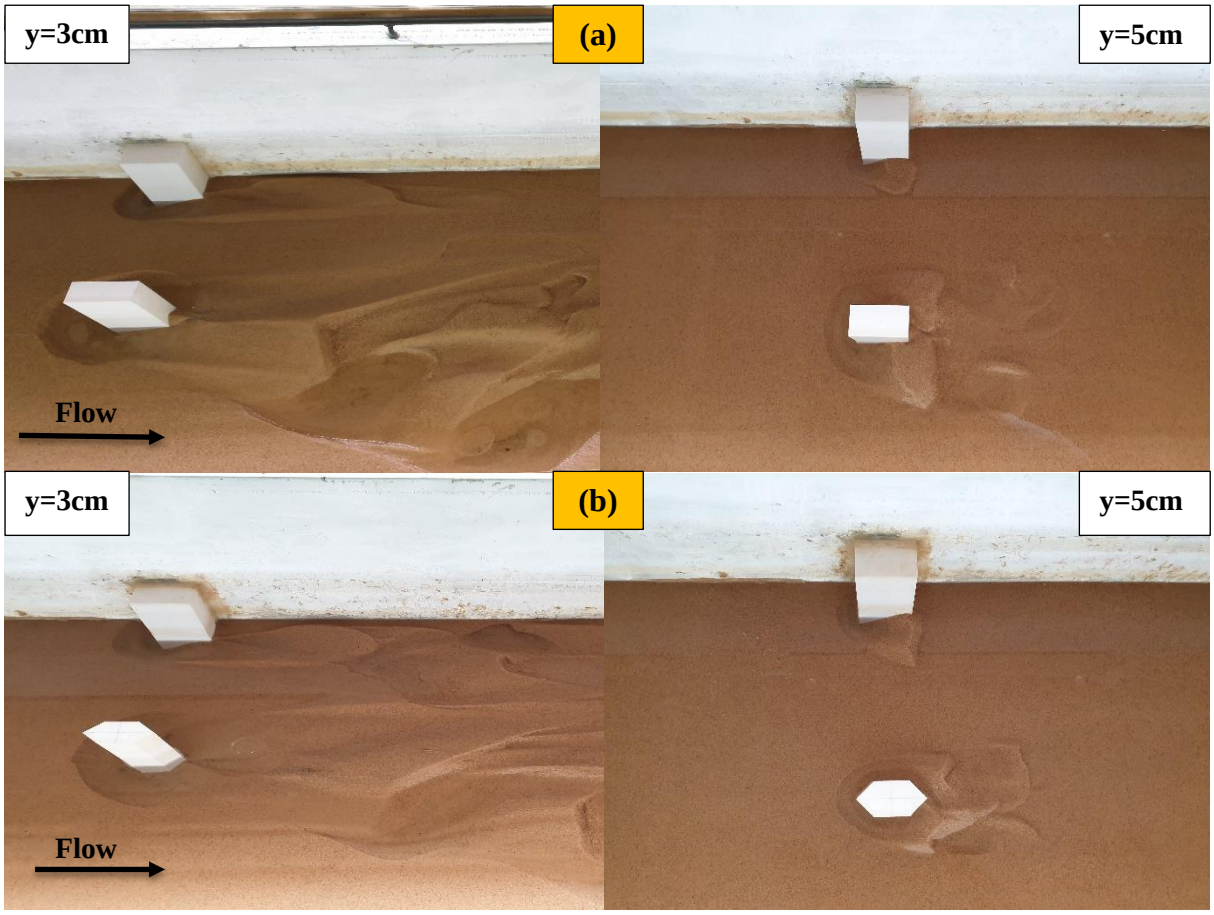

Figure 14. Photos display the impact of flow depth (y) on scouring process at (X=23.75cm and Q=3.77 L/sec) for (a) rectangular pier with abutment and (b) ogival pier with abutment.

3.5 Effect of pier geometry on scour depth (ds)

As can be seen from experiments results, the maximum scour depth that caused by rectangular shape was more than ogival shape by a percentage about (11, 12.4 and 11.2%) for spacing (X=23.75, 16, 9cm), respectively, under the same conditions of maximum Froude number (Fr). It was noticed that rectangular and ogival pier corners were the starting point of local scour development, and higher scour occurs at these corners. The pier considers as an obstruction which create stagnation zone. Thus, when high velocity effects on the pier upstream side, it will create a velocity jet which move in the downstream direction and ending in creating a scour hole. The intensity of velocity jet is a function of the flow approach velocity and exposed area of pier to the flow. For rectangular pier the exposed area of upstream face is more than ogival, and the effect of corner edge sharpness made scour hole development higher at rectangular than ogival shape. Figure 15 shows the comparison between scour depth for rectangular and ogival pier at different parameters.

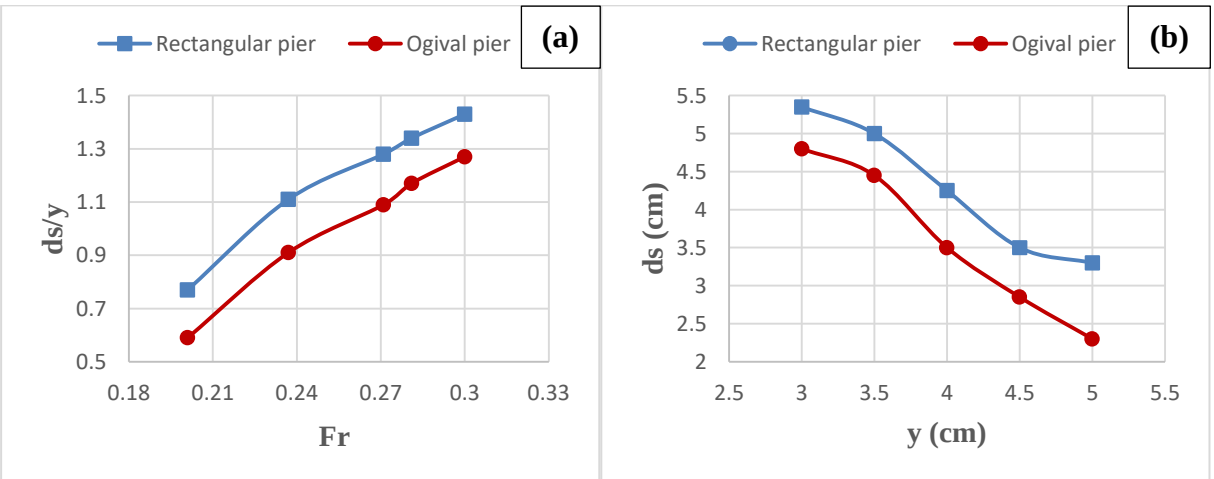

Figure 15. Effect of pier geometry on scour depth at different parameters and constant spacing (X=23.75cm) (a) Froude number and (b) flow depth (y).

4. Conclusions

The conclusions summarized from the present study are as follows:

(1) From laboratory observations, the scour process started to develop near the corners (sharp edges) of rectangular and ogival pier, where the maximum scour depth found to be near these corners. And almost more than 50% of pier scour depth developed during the first hour of the experiments time.

(2) The effect of several parameters on the scour hole around the pier and abutment was studied. The results acquired showed that the scour depth increasing when increasing flow intensity and Froude number. While the increasing in flow depth (y) could decrease the dimensions of scour depth.

(3) The impact of spacing (x) between pier and abutment was investigated and the results showed that when reducing the spacing, the scour depth increased for the pier while decreased for abutment due to the interference of horseshoe vortex between the two structures.

(4) At maximum Froude number, the increasing percentage in the scour depth was measured to be (5%) for rectangular and (3.4%) for ogival when reducing spacing (from 23.75 to 16cm), while (7%) and (6.7%) for rectangular and ogival, respectively for spacing reduced (from 23.75 to 9cm). Moreover, the decreasing percentage for abutment ranged between (10.8% to 22.2%) under the same value of maximum Froude number.

(5) Reducing spacing between pier and abutment not only affect the scour depth readings but also will impact the location of bed material depositions at the downstream. In which, the bed sediment tends to

depose in the opposite direction (i.e. when reducing the spacing between pier and abutment on the right side of the flume, the deposition location tends to the left side) as seen in figure 11 and 12.

(6) The scour depth occurs around rectangular pier was more than ogival pier by percentage (11, 12.4 and 11.2%) for spacing (23.75, 16 and 9cm), respectively. So it can be concluded that the pier geometry plays an effective role in reducing the scour phenomenon.

(7) Although the pier and abutment models have the same sharp edges and were under the same flow conditions during the experiments, but the results showed that the pier scour depth was higher than abutment scour depth. This is due to the effect of the wall flume on reducing the flow velocity near the abutment.

5. References

[1] Xiong W, Tang P, Kong B and Cai C S 2016 Reliable bridge scour simulation using eulerian two-phase flow theory *J. Comput. Civ. Eng.* **30** 1-11
[2] Meyering H 2012 Effect if sediment density in bridge pier scour experiments PhD Thesis University of Braunschweig-Institute of Technology and Faculty of Engineering, University of Florence, Germany
[3] Alabi P D 2006 Time development of local scour at a bridge pier fitted with a collar M.Sc. Thesis Department of Civil and Geological Engineering, University of Saskatchewan, Saskatchewan, Canada
[4] Lu J Y, Hong J H, Su C C, Wang C Y and Lai J S 2008 Field measurements and simulation of bridge scour depth variations during flood *J. Hydraul. Eng.* **134** 810-21
[5] Bridge Scour Manual 2018 *Supplement to Austroads Guide to Bridge Technology: Bridge Scour* (Queensland: Australia, Department of Transport and Main Roads) part 8 chapter 5
[6] Cheremisinoff N P and Cheng S L 1987 *Hydraulic Mechanics 2 Civil Engineering Practice*, (Technomic Published Company, Lancaster, Pennsylvania, U.S.A.) 780p
[7] Melville B W and Coleman S E 2000 *Bridge Scour-Water Resources publications* (Highlands Ranch: Colorado)
[8] Wang C, Yu X and Liang F 2017 A review of bridge scour: mechanism, estimation, monitoring and countermeasures *Journal of International Society for the Prevention and Mitigation of Natural Hazards* **87** 1881-1906
[9] Liu S, Yang Y and Wu X 2017 Simulation of local scour around a cylindrical bridge pier and a semicircular abutment using unsteady k-ع model combined with σ-grid *Open Civ. Eng. J.* **11** 598-614
[10] Muzzammil M, Gangadharaiah T and Gupta A K 2004 An experimental investigation of a horseshoe vortex induced by a bridge pier *Proceedings of the Institution of Civil Engineers-Water Management* **157** 109-19
[11] Shen H W, Schneider V R and Karaki S 1969 Local scour around bridge piers *J. Hydraul. Eng.* **95** 1919-41
[12] Zhang H and Nakagawa H 2008 Scour around spur dyke *J. Adv. Res.* **51** 633-52
[13] Chiew Y M and Melville B M 1987 Local scour around bridge piers *J. Hydraul. Res.* **25** 15-26
[14] Richardson E and Davis S 2001 *Evaluating Scour at Bridges* (Federal Highway Administration U.S.)
[15] Melville B W 1997 Pier and abutment scour: integrated approach *J. Hydraul. Eng.* **123** 125-36

Acknowledgments

We acknowledge that all the hydrological data was acquired from the laboratory of hydraulic in Civil Engineering Department, Basrah University.